

Sensing of gaseous atmospheric pollutants by DIAL technique in the IR spectral region

Yu.M. Andreev, P.P. Geiko, and I.V. Samokhvalov*

**Tomsk State University
Institute of Optical Monitoring,
Siberian Branch of the Russian Academy of Sciences, Tomsk*

Received June 4, 2003

The paper summarizes basic results on the development of differential absorption lidar (DIAL) systems with homemade laser sources that have been carried out at the Institute of Atmospheric Optics SB RAS, Siberian Physical-Technical Institute, Institute of Optical Monitoring SB RAS, and Radio-Physical Department of Tomsk State University since 1974. Field tests of lidar gas analyzers and measurements of the gas composition of the atmosphere are presented.

Introduction

As known, at remote determination of the composition and state of the atmosphere with high spatial resolution and sensitivity, maximum information can only be obtained using optical methods employing sources of coherent radiation. The differential absorption lidar (DIAL) method in the shortwave part of the mid-IR (2.5–14 μm) has the highest potentialities and gives best practical results in determination of concentrations of the gaseous atmospheric constituents. It is just this spectral range that includes intense isolated absorption lines and spectral structures of almost all atmospheric gases that are suitable for measurements. This range is also attractive for sensing of coarse fractions of natural and industrial aerosols. Ideally, the combined monitoring of atmospheric aerosol requires measurements to be conducted in all atmospheric transmission windows in the range from 0.2 to 14 μm . The UV spectrum and the adjacent part of the visible spectrum are promising for monitoring of fine special and natural aerosols, as well as some gaseous constituents, such as O_2 , SO_2 , NO and other nitrogen compounds. Finally, the submillimeter and millimeter spectral ranges are good for sensing gaseous composition of the atmosphere because of the presence of intense, spectrally resolved lines of almost all atmospheric gases.

In practice, in starting the development of sensing facilities (lidar systems) at the Institute of Atmospheric Optics SB RAS and Radio-Physical Department of the Tomsk State University early in the 1970s, covering not only such a wide range, but even its parts was restricted by the lack of needed sources of radiation. The solid-state, first of all, ruby and Nd lasers available commercially permitted development of the basic versions of aerosol lidars employing these sources. Before the early 1980s, industrial and research companies gradually put tunable dye lasers operating in the visible range into production and markedly progressed in the development of UV excimer lasers and frequency

converters for laser radiation from the visible and near-IR regions into the UV region. These sources immediately found wide use in lidars.

The situation with the mid-IR region was most difficult. Only CO_2 lasers operating in the region from 9.2 to 10.8 μm turn out suitable for this application. In parallel with the use of CO_2 lasers, breakthrough, for that time, optical parametric oscillators (OPO) based on nonlinear crystals were developed. However, low performance characteristics of the OPOs did not allow then any significant results to be obtained in analysis of gaseous constituents of the atmosphere. It is just the lack of sources of radiation needed that still impedes the development of lidar gas analyzers operated in the mid-IR region. This situation automatically put the priority onto the development of radiation sources, as new versions of lidars always follow the advent of new sources of radiation.

Consider the history and key results of the development of lidar gas analyzers for the mid-IR, as well as intermediate results of designing new radiation sources for traditional and upcoming femtosecond and mobile lidars. Now let us consider the DIAL method.

1. DIAL method

This method is based on the most effective interaction of optical radiation with molecules of atmospheric gases, namely, resonance absorption, that primarily determines the main advantages of technical facilities that employ this method: high sensitivity in real time and spatial resolution sufficient for long-range remote measurements. Depending on the problem formulated, photodetectors in DIAL gas analyzers record optical echoes from special reflectors or radiation diffusely reflected by topographic targets: trees, buildings, hills, etc. These are open-path meters and so-called TT lidars operating using topographic targets. The latter enable one to determine path-averaged concentrations of gases by comparing the signals received at the wavelengths within an

absorption line of a gas under study and lying in the neighboring atmospheric transmission window. If atmospheric aerosols are used as distributed reflectors, then we can speak about differential absorption and scattering (DAS) lidars that enable one to determine the concentration profiles of a gas under control.

The power of a lidar echo reflected from atmospheric aerosols is described by the lidar equation

$$P(\lambda, R) = P_L \frac{A_0}{R^2} \xi(\lambda) \beta(\lambda, R) G(\lambda, R) \frac{c\tau}{2} \times \exp\left(-2 \int_0^R k(\lambda, R') dR'\right), \quad (1)$$

where $P_L = \frac{1}{\tau} \int_0^\tau P(t) dt$, $P(t)$ and τ is the time

distribution of power and duration of the sensing pulse; A_0 is the area of the receiving telescope; R and $\beta(\lambda, R)$ are the range and the coefficient of backscattering of the scattering volume; $\xi(\lambda)$ is the transmittance of the lidar optics; $k(\lambda, R)$ is the total atmospheric extinction coefficient, $G(\lambda, R)$ is the

lidar geometrical factor; $\exp\left(-2 \int_0^R k(R') dR'\right)$ is the

atmospheric transmission along the sounding path to the scattering volume and back. To determine the concentrations averaged over the sensing path in Eq. (1), we have to substitute ρ/π for $\beta(\lambda, R)c\tau/2$, where ρ is the reflection coefficient of the used reflector or object. The total extinction coefficient for the sensing radiation is

$$k(R, \lambda) = N(R)\sigma(\lambda) + \kappa_c(\lambda, R) + \kappa_a(\lambda, R) + \sum_{i=1}^m k^{(i)}(\lambda), \quad (2)$$

where $N(R)$ and $\sigma(\lambda)$ are the gas concentration and absorption cross section; $\kappa_c(\lambda, R)$ and $\kappa_a(\lambda, R)$ are the absorption coefficient of the water continuum and the aerosol extinction coefficient, $k^{(i)}(\lambda)$ are the absorption coefficients of interfering gases. In the mid-IR, extinction due to molecular scattering is weak as compared to the aerosol extinction. After calculation of the log power ratio of on (at λ_1) and off (at λ_2) an absorption line signals and its differentiation assuming that measurements are conducted in the "frozen" atmosphere (measurement time less than 0.1 ms), when the aerosol scattering coefficient and the water vapor continuum absorption coefficient along the sensing paths shorter than 3–5 km can be thought fixed functions of the distance to the lidar, the mean content of the gas under study in the layer $\Delta R = R_2 - R_1$ (ppb) can be determined as

$$N(R_1, R_2) = \frac{1}{\Delta R} \int_{R_1}^{R_2} N(R') dR' = \frac{10^9}{2k_{12}\Delta R} \times$$

$$\times \left[\ln \frac{P(\lambda_2, R_1)P(\lambda_1, R_2)}{P(\lambda_1, R_1)P(\lambda_2, R_2)} + \ln \frac{G(\lambda_1, R_1)G(\lambda_2, R_2)}{G(\lambda_1, R_2)G(\lambda_2, R_1)} - \Delta R \left\{ [k_c(\lambda_1) - k_c(\lambda_2)] + [k_a(\lambda_1) - k_a(\lambda_2)] + \sum_{i=1}^m k_{12}^{(i)} \right\} \right],$$

where $k_{12}^{(i)} = k^{(i)}(\lambda_1) - k^{(i)}(\lambda_2)$ is the differential absorption coefficient of the i th gas. Because of the frozen atmosphere assumption, the differential absorption cross section of gases $\sigma_{12} = \sigma(\lambda_1) - \sigma(\lambda_2)$ is replaced by the differential absorption coefficient $k_{12} = \sigma_{12} N_L$, where N_L is the Loschmidt number. In our lidar systems, the differential absorption coefficient of the gas under study and interfering gases, as well as the water vapor continuum absorption coefficient are determined using the available data banks of spectral line parameters (e.g., HITRAN) and involving the data on the atmospheric temperature and pressure from standard weather stations. The aerosol extinction coefficients are chosen from the known atmospheric models. The measurement error is determined as

$$\frac{\delta_N^2}{N^2} = \frac{1}{M} \left\{ \frac{\delta_\sigma^2}{\sigma_{12}^2} + \delta_B^2 + \delta_J^2 + \delta_C^2 + \delta_A^2 + \delta_F^2 + \frac{1}{4\sigma_{12}^2 N^2 \Delta R^2} \left[4 \frac{\delta_p^2 - \text{cov}[P(R), P(R + \Delta R)]}{P^2(R)} \right] \right\}, \quad (4)$$

where M is the number of laser pulses; δ^2 are variances of different parameters;

$$\text{cov}[P(R), P(R + \Delta R)] = 2\delta_p^2 \{ \sin(2\pi\Delta f 2\Delta R / c) / (2\pi\Delta f 2\Delta R / c) \}$$

is the covariance of lidar returns from the scattering volume R , $R + \Delta R$; Δf is the passband of the lidar electronic system. In addition, the following designations are used:

$$B = \ln \frac{\beta_{11}\beta_{22}}{\beta_{12}\beta_{21}}; \quad J = \ln \frac{G_{11}G_{22}}{G_{12}G_{21}}; \quad C = -k_{12}^c \Delta R; \quad (5)$$

$$A = -k_{12}^a \Delta R; \quad F = -\Delta R \sum_i k_{12}^{(i)}.$$

The spectral dependence of the total scattering coefficient and the aerosol backscattering coefficient on the frequency ν of laser radiation is determined as

$$\delta_A^2 = \bar{k}^a{}^2 \left(4 \frac{\Delta \nu}{\nu} \right)^2 \Delta R^2; \quad \delta_B^2 = \left(4 \frac{\Delta \nu}{\nu} \right)^2. \quad (6)$$

The geometrical factor is calculated carefully by the geometric optics methods. To check the correspondence and exclude unexpected errors, the backscattering signal at the wavelengths off the gas absorption lines was compared with the results of estimation.

2. Open-path meter based on CO₂ laser

As follows from estimates by Eq. (1), open-path measurements with the use of retroreflectors can be carried out using microwatt radiation sources, while the measurements with the use of topographic targets require the sensing pulse energy from tenths to few millijoules. Spatially resolved measurements are possible only at the pulse energy up to some fractions, units, and even tens of joules at transition from the short-wave part of the mid-IR to the region covered by CO₂ lasers. In the 1970–1980s the main difficulties in the development of gas analyzers covering the region under study consisted not only in production of powerful and reliable tunable sources of radiation. Because of the lack of radiation visualizers and matrix detectors, the most difficult problem was the formation and precision control of spectral parameters of narrow lines. Thus, in the surface atmosphere the spectral width of laser lines should not exceed, at least, 1/3 of the absorption line width, which is 0.003 to 0.03 cm⁻¹. Stabilization and the accuracy of control of line position should be characterized by even smaller values.

At that time, CO₂ lasers were found to be most suitable for application in lidars. Due to their relative simplicity and reliability, as well as high energy and performance characteristics, including the smooth and quasi-equidistant spectrum, these lasers permit home development, maintenance, and modernization.

The main advantages of CO₂ lasers are easy control of the spectral parameters of radiation and no need in their formation. At the typical working mixture pressure of 18 Torr in low-pressure lasers, the spectral width of laser lines, even in the absence of any tools for stabilization of the output power, cavity length, modal composition of the radiation is about $2 \cdot 10^{-3}$ cm⁻¹ as narrow. At the typical cavity length of about 1 m and operation in the TEM₀₀ mode, the laser spectrum includes 3–4 longitudinal modes, whose instability in the amplitude and frequency does not affect the results of measurements because of a narrow spectral width of the laser line and the reference channel present in lidars. The spectral position of some laser lines is fixed by the parameters of the working mixture and is known very accurate. Fifty to ninety laser lines are separated by 1.5–2 cm⁻¹, which allow their easy selection and assignment with the use of diffraction gratings controlled with a stepper motor. In the case of TEA CO₂ lasers, the spectral width of laser lines is about 0.1 cm⁻¹, which is quite acceptable for applications to atmospheric studies.

The tuning range of CO₂ lasers includes absorption lines of more than 90 various gases, in particular: NH₃, C₂H₂, H₂O vapor, O₃, CO₂, N₂O, NO₂, HNO₃, SF₆, OSC, CS₂, freons, organic gases, hydrazine, rocket propellants, poison gases. Of practical significance are the first three low-molecular gases. Due to high absorption cross sections within the lines that are spectrally close to

laser lines and because of rather high contents in the urban atmosphere, they can be monitored with high accuracy. High-molecular gases and vapors can be monitored reliably only in the case that their number is within a few tens. The possibility of monitoring of ten such constituents at their simultaneous presence in the atmosphere is quite doubtful because of overlapping of the absorption spectra. Hence, it is obvious that the main disadvantage of the CO₂ lasers is their limited spectrum.

The capabilities of an open-path meter based on a low-pressure tunable CO₂ laser with the use of a retroreflector made by 1974 following a traditional optical arrangement in parallel with foreign devices have been described in Ref. 1. With the 9P(8) line used the accuracy of measurement of the diurnal behavior of the O₃ content was 8–9 ppb at the path length of 2.5 km, and that for ethylene was 3 ppb with the use of the 10P(14) line. Ammonia was measured with the accuracy of about 1 ppb at the 9R(30) line, and the content of benzene and acrolein in automobile exhausts was evaluated.² The disadvantages of this meter were low (0.1%) accuracy of measurement of electric signals and the lack of systems for stabilization of the cavity length, which lead to lasing failures and appearance of two to three operating modes because of the cavity misalignment. The first attempt of using a TEA CO₂ laser for gas analysis of the atmosphere yielded no expected result because of its low performance characteristics.³

3. TT lidar based on CdSe OPO

The first, known from the literature, DIAL system operating in the mid-IR with the use of frequency converters was made and tested in 1977–1978 (see Ref. 4). As a radiation source, it employed a CdSe OPO pumped by Er³⁺:YAG (2.96 μm) and cryogenic Dy²⁺:CaF₂ (2.36 μm) lasers with two amplification cascades, which operated in the ranges of 2.8–4.2 and 7.5–13.7 μm with the line width of 1 cm⁻¹. At the OPO efficiency of 1–10% in a nonlinear CdSe crystal 40 mm long, the peak power of 30–40 ns pulses exceeded 100 kW at the pulse repetition frequency up to 10 Hz, and the energy was 3–4 mJ. This OPO meets most of the requirements imposed on the lidar radiation sources; therefore, already in the first experiments the gas analyzer based on it has demonstrated the principle possibility of measuring the concentrations of NH₃, CH₄, CO, and HCl at the health-safe level when operated in the TT mode at the path length of 0.1–1.0 km. However, two-year operation of OPO showed its low performance characteristics. The maximum number of pulses between failures did not exceed several hundreds.

The experience of operating the first two lidars developed showed the promises of the methods of nonlinear crystal optics for extending the possibilities of gas analysis. The low efficiency of nonlinear crystals revealed the need in new crystals, and the complexity of the OPO construction indicated that it is preferable to use the second and third harmonic

generators, as well as harmonic mixers for CO₂ laser radiation, rather than the threshold OPO frequency converters. Note that the wavelength of the CO₂ laser radiation and its harmonics fall just into the atmospheric transmission windows in the ranges of 2.0–2.5, 3.0–4.2, 4.4–5.0, and 8–14 μm.

An extra factor stimulating the development of harmonic generators is that the accompanying degradation of the energy parameters is compensated for by the increasing sensitivity of the radiation detectors. Thus, the energy loss at even relatively low SHG efficiency of about 10–20% is almost totally compensated for by the increase in sensitivity of InSb detectors in the 5-μm range. It is at least 5 times higher than that of HgCdTe detectors of CO₂ laser radiation (detectability of 10¹¹ vs. 2·10¹⁰ cm·Hz^{1/2}/W). The InAs detectors of third-harmonic exceed by 5 times the sensitivity of InSb detectors of the second harmonic radiation.

4. Open-path meter based on CO₂ laser with SHG

Figure 1 depicts the modernized Rezonans-3 gas analyzer³ mounted in a trailer and equipped with a frequency doubler based on the ZnGeP₂ crystal grown at Siberian Physical-Technical Institute in the group under the leadership by Voevodin and applied for the first time.⁵

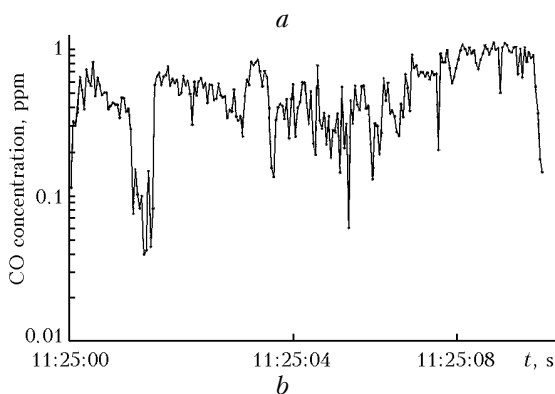
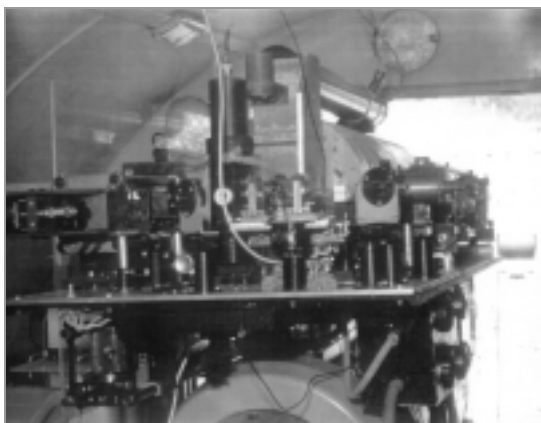


Fig. 1. The external view of the open-path gas analyzer with ZnGeP₂ frequency converter (shown by arrow) (a) and evolution of the CO concentration at a highway as estimated at the second harmonic wavelength.

Two-month field tests confirmed the improved capabilities and high performance characteristics of the gas analyzer. The diurnal behavior of the carbon monoxide content was measured (Fig. 1b) at the wavelength of the second harmonic of the 9R(18) line positioned at $\nu = 2154.604 \text{ cm}^{-1}$ and coinciding with the R(2) line of the CO fundamental band with the position at $\nu = 2154.596 \text{ cm}^{-1}$ and the absorption coefficient of $29.7 \text{ cm}^{-1} \cdot \text{atm}^{-1}$ (Ref. 6).

The absence of cryogenic cooling of ZnGeP₂, unlike CdGeAs₂ single crystals used abroad, simplified the lidar construction, and its high threshold to optical damage provided for non-failure operation during many-month measurement cycles under field conditions. This was also favored by application of MOS *n*-InSb structures with low threshold power of $10^{-13} \text{ W/Hz}^{1/2}$ as radiation detectors in measurements at second harmonic wavelengths that permitted operation with radiation, whose power is two to three orders of magnitude lower than that needed for InSb photodiodes. Complete interception of the sensing beam by the optical-mechanical receiving system at the retroreflector spaced by up to 1.5 km, installation of the gas analyzer onto jacks isolated from a cab, and a large ($\varnothing 8 \text{ mm}$) photosensitive area of the MOS structure excluded the effect of vibrations, atmospheric turbulence, and parallel shear of SH radiation at fine angular adjustment of the crystals. At the path length of 2 km, the measurement accuracy was 4% of the background concentration equal to 100 ppb. Before the beginning of measurements, the meter transmittance is calibrated by installing the retroreflector just near the transceiver and measuring the calibration coefficient at the working wavelengths, as in the case of 100% transparency of the atmosphere. Then a 2-m long cell with known amount of the gas under study is installed on the path to refine, if necessary, absorption cross sections and to absolutely calibrate the meter.

The equipment for recording and preprocessing the data on a computer operated in real time. The high content and the absorption coefficient of carbon monoxide allowed its content to be monitored with the use of topographic targets as reflectors. The CO₂ laser operated in the repetitively pulsed mode with the pulse repetition frequency of 1 kHz and the peak power of 1–3 kW, and its radiation was frequency doubled with the 5% efficiency. In using topographic objects spaced by up to 500 m and cryogenic InSb photodiodes, the signal-to-noise ratio at one-minute signal accumulation achieved 100 and allowed monitoring of the background and higher than background content of CO (Ref. 7). It was found that 20-m long path is sufficient for monitoring of the pollution level typical of highways.

The list of gases sensed at the SH wavelengths includes OCS with the use of the absorption line at $2082.5596 \text{ cm}^{-1}$ with the intensity of $1.17 \cdot 10^{-19} \text{ cm}^2/(\text{mol} \cdot \text{cm})$, which coincides with the second harmonic of the 9P(26) laser line accurate to 0.0013 cm^{-1} , as well as NO with the use of the line

doublet at 1871.066 and 1871.055 cm^{-1} each with the intensity of $1.72 \cdot 10^{-20} \text{ cm}^2/(\text{mol} \cdot \text{cm})$, coinciding with the SH of the 10P(27) line of the $^{12}\text{CO}_2$ laser with the accuracy of 0.01 and 0.02 cm^{-1} . Examples of NO measurements under field conditions can be found in Ref. 8.

5. Open-path meters based of CO_2 and CO laser frequency mixers

Introduction of the second CO_2 laser into the structure of an open-path meter and the use of the available second harmonic generator to shift the radiation frequency for the both lasers allowed improving the measurement accuracy and extending the list of gases monitored.^{7,8} At generation of all versions of the sum frequencies, the number of frequency-converted lines increases 40 times, which permits selection of an optimal line from a dozen of possible versions, for example, in the case of CO monitoring using the above absorption line. The obtained density of Raman lines is sufficient to determine the profile of an absorption line and, consequently, gas temperature and pressure. The further increase of the number of monitored gaseous constituents is possible due to the use of generators of higher harmonics and Raman frequencies of CO and CO_2 laser radiation, fundamental radiation of the first CO_2 laser and second harmonic of the second CO_2 laser. In the latter case, for example, the minimum detectable concentrations of some hard-to-monitor pollutants of the real atmosphere are about a few ppb at 1-km long near-surface measurement path. In particular, it is 3 ppb for HCl at measurements at the sum frequency of the second harmonic of 10P(26) line and 10P(20) line or $2 \cdot 10P(26) + 10P(20)$ and with the Raman line $2 \cdot 10P(26) + 10P(14)$ used as a reference one, which gives the differential absorption coefficient $\Delta = 34 \text{ cm}^{-1} \cdot \text{atm}^{-1}$. For CH_4 it is 2 ppb if using $2 \cdot 9P(10) + 10R(18)$ and $2 \cdot 9R(16) + 10P(32)$ with $\Delta = 43.7 \text{ cm}^{-1} \cdot \text{atm}^{-1}$, and it is 6 ppb for PH_3 with the use of $2 \cdot 9P(28) - 9R(34)$ and $2 \cdot 9P(34) - 9R(12)$ with $\Delta = 20.4 \text{ cm}^{-1} \cdot \text{atm}^{-1}$. In such a case, the restriction on the number of monitored gases is apparently lifted. Measurements of the N_2O concentration at the sum frequency of the lines 9R(40) and 9R(18) of two CO_2 lasers accurate to 15 ppb at the path length of 2 km are shown in Ref. 8. The possibility of measuring CO_2 and NO_2 content was demonstrated under laboratory conditions. The next modernized model of the open-path meter, which included three tunable lasers: two CO_2 lasers and one CO laser, with a set of ZnGeP_2 frequency converters, is described in Ref. 9.

6. Lidar gas analysis

To monitor the atmosphere above extended areas in real time, carry out combined basic investigations, and train specialists and personnel dealing with lidars, a mobile lidar system permitting realization of all possible versions of

DIAL systems (Fig. 2) was produced in 1993–1996.^{10–12}

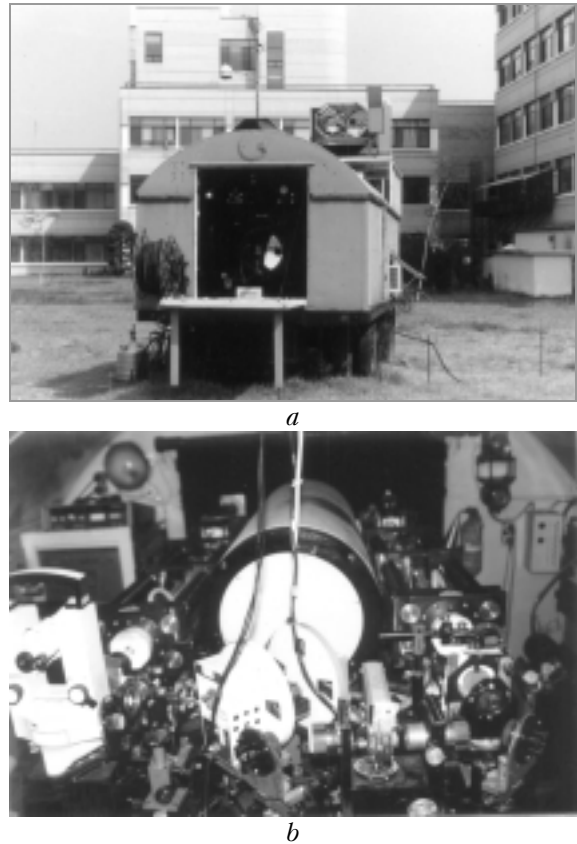


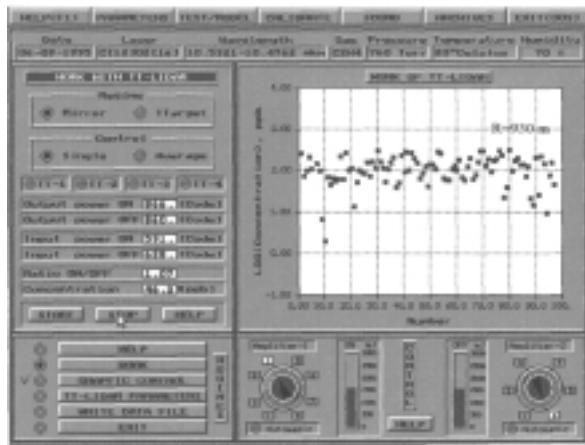
Fig. 2. The external view of the DIAL system: transceiver part of the two-mode lidar (on the roof) (a) and external view of the open-path gas analyzer (front view through an open hatch) inside a trailer (b).

It consists of an independently operated open-path gas analyzer and a tunable lidar operated using topographic objects or in the mode of recording the return signals scattered in the backward direction by atmospheric aerosols. In both of the cases, a 500-mm-diameter aspherical tunable Cassegrain–Newton receiving system with the effective focal length of 1840 mm is used, and 80% of energy of the recorded signal is focused into a spot of 60 μm in diameter. In this model, two original homemade CO_2 lasers with ZnGeP_2 frequency mixers are used. A massive (80 kg) rigid frame on four 40-mm invar rods along with the active slow magnetostrictive and fast piezoelectric fine tuning ensures efficient passive stabilization of the cavity length. At additional selection of TEM_{00} mode and the proper pump level provided for by use of a highly stabilized power supply, the spectral width of the laser line decreased from $2 \cdot 10^{-3}$ to $6 \cdot 10^{-6} \text{ cm}^{-1}$, which corresponds to the width of a single longitudinal mode stabilized at the center of a luminescence line. A gas quartz cell and a photoacoustic detector used permitted investigation of the local content of gaseous atmospheric constituents and determination of the absorption cross sections for model conditions all over the

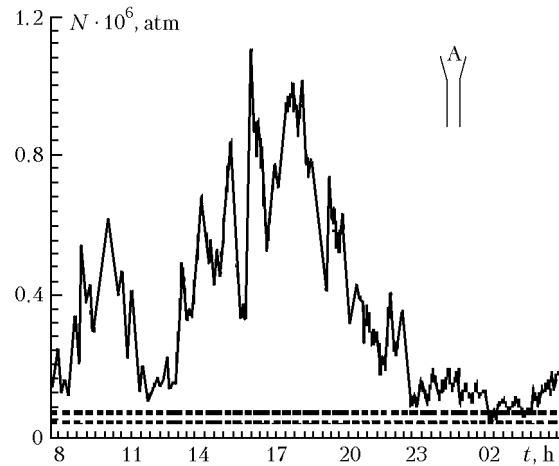
atmospheric depth. In the case of recording return signals backscattered by aerosols, the lidar employing the biaxial scheme was operated in the direct detection mode. It includes two tunable repetitively pulsed TEA CO₂ lasers with the pulse energy of 1–4 J, line spectral width of 0.1 cm⁻¹, pulse repetition frequency of 0.2–4 Hz, first peak duration of a pulse of 40–120 ns, and pulse tail of 0.1–3 μs with the ratio of its energy to the total energy up to 25% regulated by proper selection of the active medium and supply mode. The lasers emitted a couple of pulses at different wavelengths with the lag of about 1–3 ms.

Using model estimates based on the results of previous measurements, the lidar geometrical factor optimal for the problem to be solved is selected before the beginning of operation. Then it is set due to the foreseen capability of controlled variation of all geometrical parameters of the lidar transceiver system: field of view of the receiving and transmitting optical systems, their convergence

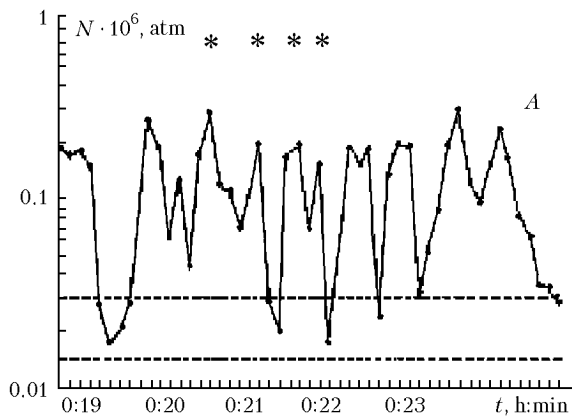
angles, basic separation and effective focal lengths, as well as parameters of sensing beams. Before operation in the TT mode, the reflection coefficients of topographic objects were studied. It was found that their values range from 0.1–0.2% (grassed hill slopes, tree crowns) to 5–7% (rocks, unpolished metal plates, building walls). The control and processing system was based on a PC 486 computer and had programmable amplifiers and 12-bit 1-MHz ADC. This system checked the state of individual units and the lidar as a whole before and after measurement cycles, took into account real weather parameters of the atmosphere, calculated expected lidar parameters for every particular measurement cycle and, whenever necessary, compared them with the real parameters and/or parameters of other known lidars, processed measurement results in real time and after measurements, and stored them. Both parts of the lidar system had optical tables and optical-mechanical units that allow realization of any known version of a local meter.



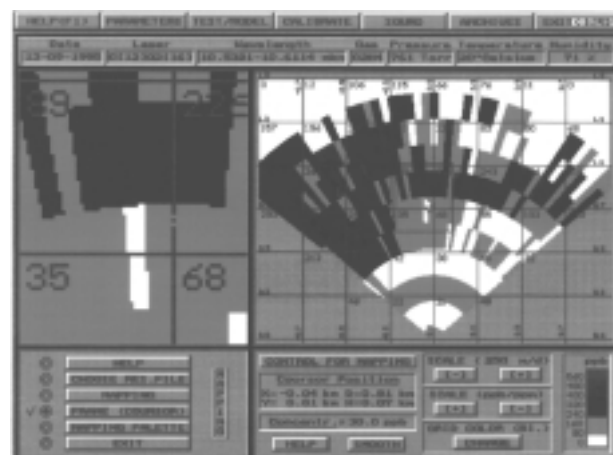
a



b



c



d

Fig. 3. Variations of ethylene concentration in the atmosphere of the city of Taejon, South Korea: data of open-path measurements with topographic targets used as reflectors in real time (a), after the final processing for 24 hr (b), and during nighttime (c). Dashed curves show the background concentrations, asterisks mark the time of control car passages under the measurement path. The mapping results are obtained in the mode of backscattered signal recording.

The field tests of the lidar system were carried out in KAIST (Taejon, South Korea). The range in operation against topographic targets achieved 10–15 km, and the maximum range, from which backscattered signals were recorded, was 5 km with the spatial resolution of 150–200 m. The measurement results were displayed on a monitor in real time. Figure 3a depicts, in particular, the results of measurement of the C₂H₄ content at operation in the TT mode.

Archiving and following processing of measurement data yielded both the diurnal behavior of C₂H₄ and its fast variations for short periods (Figs. 3b and c).

At operation in the DAS mode and scanning over the angle of elevation and height, two-dimensional maps of pollutant distribution with topographic reference were drawn (Fig. 3d). The main sources of errors in measurements are fast variations of the recorded signals that hamper their smoothing, incorrect knowledge of the aerosol backscattering coefficient, and electromagnetic interference. If operating using targets spaced by 3 km, the signal-to-noise ratio up to 10 000 was obtained for one pair of shots. At the path length of 3 km, the accuracy in determination of concentrations was 1–10 and 20–80 ppb at open-path measurements and at operation using a topographic target, and 20–100 ppb/km in the case of backscattering.

7. Uncalled and promising sources of radiation for lidar systems

Because of financial problems, some lidar models based on original sources of radiation developed since the early 1990s have remained unrealized. They include a CO₂ laser operating simultaneously in the fundamental and hot 9- and 10- μ m bands, as well as in the 4.3- μ m band and at individual lines in the region of 2–3 μ m at the inert gases added to the active medium with a set of frequency converters: generators of harmonics and Raman frequencies for all laser lines. The frequency-converted spectrum covered the region of 2–12 μ m, which is highly competitive with the lasing region of broadband OPOs, with the density up to 10⁻³ cm⁻¹. Application of such a source for gas analysis of the surface atmosphere is identical to the use of a smoothly tunable source.¹³ A generator of submillimeter radiation has also been left uncalled. It operated with frequency tuning in the region of 102.6–110.76 μ m and was a difference frequency generator for different pairs of lines of a two-frequency TEA CO₂ laser.¹⁴ The same happened with up-converters of mid-IR laser radiation into the near-IR region, which were capable of improving the signal-to-noise ratio of lidar photodetectors by two to three orders of magnitude.¹⁵

In recent years, the physical properties of poorly studied nonlinear crystals HgGa₂S₄ and LiInS₂, new LiInSe₂ crystals, and new mixed AgGaGeS₄ crystals from the AgGa_{1-x}Ge_xS₄ family at $x = 0.5$ and

Hg_{0.65}Cd_{0.35}Ga₂S₄ from the Hg_(1-x)Cd_xGa₂S₄ family have been investigated. Their applicability to the development of more efficient, as compared to the known crystals, and original sources of radiation for lidar systems was demonstrated.^{16,17} Thus, at doubling the CO₂ laser frequency, the HgGa₂S₄ and Hg_{0.65}Cd_{0.35}Ga₂S₄ crystals showed the efficiency threefold as high as that of ZnGeP₂. All the above crystals are useful for efficient mid-IR OPOs pumped by solid-state lasers, in particular, by the Nd:YAG laser for the first time, because their transparency range begins from the wavelength of 0.4–0.6 μ m and ends nearby 12.5–16.5 μ m. It was shown that further improvement of the technology of growing high-quality doped GaSe:In crystals would allow the same conclusion to be drawn for them. The use of frequency converters for Nd:YAG laser frequency into the mid-IR region in combination with the available commercial LBO, KTA, KTP, and BBO frequency converters for these lasers into the UV region allows production of sources of coherent radiation in the region of 0.2–12.0 μ m. Such sources can be used for development of versatile gas-aerosol lidars. Peculiarities of the transmission spectrum and high nonlinear properties allow development of difference frequency generators of microchip Nd:YAG and semiconductor lasers for portable microlidars. Biaxial LiInS₂, LiInSe₂, and AgGa_{1-x}Ge_xS₄ crystals demonstrate high potentiality in direct conversion of the frequency of available femtosecond lasers into the mid-IR and their use for development of femtosecond lidars.

Conclusion

Based on the results presented in this paper we can conclude that the concept developed for production of mid-IR lidar gas analyzers and the main directions of its realization for atmospheric monitoring are formulated rather thoroughly and deserve further development. The results obtained have obvious research and practical significance not only in the environmental protection, but also in other fields of science and technology, which require application of tunable, high-power, and reliable mid-IR radiation sources. In the further investigations, it is planned to reinforce development of versatile gas-aerosol lidars operating in the region of 0.2–14.0 μ m, as well as femtosecond and portable lidar models.

References

1. I.V. Samokhvalov, A.V. Sosnin, and G.S. Khmel'nitskii, in: *Proc. of All-Union Symp. on Radiophysical Investigations of the Atmosphere* (Gidrometeoizdat, Leningrad, 1977), pp. 78–82.
2. I.V. Samokhvalov, A.V. Sosnin, G.S. Khmel'nitskii, and S.F. Shubin, *Zh. Prikl. Spektrosk.* **32**, No. 3, 525–531 (1980).
3. A.V. Voitsekhovskii, Yu.V. Lilenko, A.S. Petrov, I.V. Samokhvalov, A.V. Sosnin, and G.S. Khmel'nitskii, in: *Remote Sensing of the Atmosphere* (Nauka, Novosibirsk, 1978), pp. 141–145.

4. Yu.M. Andreev, M.E. Karasev, V.V. Kostin, L.A. Kulevskii, V.V. Smirnov, and A.V. Sosnin, in: *Abstracts of Reports at V All-Union Symp. on Laser Sensing of the Atmosphere*, IAO SB RAS, Tomsk (1978), pp. 7–11.
5. V.E. Zuev, M.V. Kabanov, Yu.M. Andreev, V.G. Voevodin, P.P. Geiko, A.I. Gribenyukov, and V.V. Zuev, *Izv. Akad. Nauk SSSR, Ser. Fiz.* **52**, No. 6, 1142–1149 (1988).
6. Yu.M. Andreev, V.G. Voevodin, A.I. Gribenyukov, V.N. Davydov, V.I. Zhuravlev, V.A. Kapitanov, G.A. Stuchebrov, and G.S. Khmel'nitskii, *Zh. Prikl. Spektrosk.* **47**, No. 1, 15–20 (1987).
7. Yu.M. Andreev, P.P. Geiko, V.N. Davydov, V.V. Zuev, and O.A. Romanovskii, in: *Optical Properties of the Earth's Atmosphere* (TA SB AS USSR, Tomsk, 1988), pp. 132–135.
8. Yu.M. Andreev, I.L. Vasin, P.P. Geiko, S.I. Dolgii, V.V. Zuev, S.V. Smirnov, and S.F. Shubin, in: *Results of Combined Experiments "Vertikal-86" and "Vertical-87"* (IAO SB AS USSR, Tomsk, 1989), pp. 77–94.
9. Yu.M. Andreev, P.P. Geiko, V.V. Zuev, O.A. Romanovskii, and S.F. Shubin, in: *Abstracts of Reports at XIII Int. Conf. on Coherent and Nonlinear Optics* (Minsk, 1988), Part 2, pp. 221–222.
10. Yu.M. Andreev, M.Yu. Kataev, I.V. Razenkov, K.D. Shelevoi, and I.V. Sherstov, "Differential Absorption Lidar Complex," Technical Report (Tomsk–Seoul, 1996), 686 pp.
11. Yu.M. Andreev, I.A. Razenkov, and N.A. Shefer, *Atmos. Oceanic Opt.* **9**, No. 10, 905–908 (1996).
12. Yu.M. Andreev, S.V. Do, I.A. Razenkov, I.V. Sherstov, N.A. Shefer, Kh.D. Kong, and Yo.D. Pak, *Atmos. Oceanic Opt.* **10**, No. 1, 76–80 (1997).
13. Yu.M. Andreev, P.P. Geiko, A.I. Gribenyukov, V.G. Voevodin, V.V. Zuev, A.S. Solodukhin, S.A. Trushin, and V.V. Churakov, *Kvant. Elektron.* **14**, No. 10, 2137–2138 (1987).
14. Yu.M. Andreev, V.V. Apollonov, Yu.A. Shakir, and A.I. Gribenyukov, *J. of Korean Physical Society* **33**, No. 3, 356–361 (1998).
15. Yu.M. Andreev, P.P. Geiko, and V.G. Voevodin, *Atmos. Oceanic Opt.* **13**, No. 4, 370–375 (2000).
16. Yu.M. Andreev and P.P. Geiko, *Atmos. Oceanic Opt.* **15**, No. 1, 53–60 (2002).
17. Yu.M. Andreev, P.P. Geiko, V.V. Badikov, G.C. Bhar, S. Das, and A.K. Chaudhury, *Nonlinear Optics* **29**, No. 1, 19–27 (2002).